

Fermi National Accelerator Laboratory

FERMILAB-Pub-91/219-E

E665

## Calibration and Validation of a Time Of Flight Detector

T. Dreyer, M. Erdmann, J. Haas, W. Mohr, U. Seidler, G. Siegert, H. Stier and M. Wilhelm

*Fermi National Accelerator Laboratory  
P.O. Box 500, Batavia, Illinois 60510*

August 1991

\* Submitted to *Nuclear Instruments and Methods*.





# Calibration and Validation of a Time Of Flight Detector\*

T.Dreyer, M.Erdmann<sup>†</sup>, J.Haas, W.Mohr,  
U.Seidler<sup>‡</sup>, G.Siegert, H.E.Stier<sup>§</sup>, M.Wilhelm

April 16, 1991

Fakultät für Physik, Albert-Ludwigs-Universität Freiburg,  
Hermann-Herder-Straße 3, D-7800 Freiburg, Federal Republic of Germany

## Abstract

The time of flight detector of the E665 experiment at Fermilab is continuously checked and calibrated. The use of a laser calibration system enables the synchronization of individual counters and allows the correction of time shifts caused by systematic effects. With an electron test beam an average overall time resolution of 225ps was measured.

---

\*Work supported in part by the BMFT grant 5 FR 14 P

<sup>†</sup>Now at DESY, Hamburg

<sup>‡</sup>Now at PTW, Physikalisch-Technische Werkstätten, Freiburg

<sup>§</sup>Deceased

# 1 Introduction

The time of flight detector (TOF) presented in this article is part of the spectrometer used in the deep inelastic muon-nucleon scattering experiment E665 at Fermilab. Parts of the detector, originating from the EMC experiment NA9 at CERN, have been considerably improved for E665. The E665 spectrometer including some general information about the TOF hardware is described elsewhere [1]. This article gives a more detailed description of the hardware used for calibration and the offline corrections [2] of the time of flight data.

The E665 TOF detector consists of a reference counter in the beam line and two wing hodoscopes downstream of the target. The time of flight of particles measured by the detector differs due to well known systematic effects from the true time of flight. In consequence the TOF detector is provided with calibration devices to measure these effects. Calibration data are analysed offline and parametrized in order to correct the times measured. Except for one overall time offset, correction values are calculated independently of the physics data taken.

The TOF hardware is described in section two emphasising parts used for checks and calibration. The third section describes the calibration procedure. In the fourth section a brief description of the reference counter is given. In the fifth section the effects of the different corrections are shown using electron calibration data.

## 2 Hardware

### 2.1 The Hodoscopes

Each of the two hodoscope wings consists of thirty eight scintillators (NE110) covering a sensitive area of  $4.2\text{m} \times 1.6\text{m}$ . Light pulses are transmitted via guides to photomultiplier (PM) tubes (Valvo XP2020, XP2230, XP2252) on both ends of the scintillators. The tube signals are passively split. One signal is discriminated (LRS620BL) directly at the hodoscopes to supply the stop pulse for TDCs (LRS2228) which have a resolution of 100ps per count; all times are measured relative to the trigger strobe of the experiment. By digitizing the other signal in ADCs (LRS2249A) the pulse charge of the photo tube is measured.

The reference hodoscope consists of five small scintillation counters equipped with the same electronics as the hodoscope wings.

### 2.2 The Pulser and the Delay Unit

For calibration purposes the TDC modules are connected to an electronic pulser which is triggered by the TOF micro computer (see below). All TDC modules are commonly started and stopped. The stop signals are delayed using varying cable lengths switched in a CAMAC delay module (SEN PD2048). The times between start and stop signal are varied to cover the linear TDC range. By measuring the TDC mean values for different delay times the linearity of the TDC channels is checked and the individual conversion factors for counts into seconds are determined.

### 2.3 The Laser System

One of the main features of the E665 TOF detector is a laser system [3] which is used for monitoring and calibration (figure 1):

Ultraviolet light pulses are produced by a nitrogen laser. A part of the laser beam is split onto a monitoring photo tube which triggers the electronics. The intensity of the main beam can be varied by a motor driven iris diaphragm. By varying the intensity of the UV pulses in this way it is possible to measure the pulse height dependence of the time measurements, here referred to as *Time Walk*.

The laser beam is then diffusely reflected from a piece of chalk to equally illuminate a bundle of optical fibers (Quarz & Silice, PCS 200) transparent for UV light which guide the pulse to each counter. here the UV light is shifted to blue, giving a good approximation of the light produced by particles. The time spread of the pulses at the scintillators due to small differences in the length of the fibers is estimated to be less than 25ps.

The laser, the nitrogen gas supply and the diaphragm are controlled by the TOF micro computer.

### 2.4 The Micro Computer Monitoring System

The TOF is provided with a local monitoring system, based on a Motorola 68000 CPU and VME bus.

The muon beam of the Tevatron follows a spill structure. For a period of 20 seconds muons enter the experiment (*spill*). 37 seconds without beam (*interspill*) are used to calibrate and check the detectors. *Prepare For Spill* and *End Of Spill* signals are given by the accelerator. A third signal indicates the event read out of the E665 data acquisition (DA). These interrupt signals are used to synchronize the TOF micro computer, the spill timing and the E665 DA.

Figure 2 shows the TOF electronics. The ADC and TDC modules are read out via a CAMAC Read-Only-Branch of type *Romulus* [4]. All data words are collected in a *Read Only Branch Driver* (ROBD).

TDC and ADC calibration data can be read out by the micro computer from the ROBD through an *Auxiliary Crate Controller Interface* (ACCI, [5]) which interfaces to the VME bus.

In data taking mode the E665 DA system reads out the TOF data from the ROBD. A special CAMAC module (Listener) [6] was developed to analyse PHYSICS data on the micro computer. A *First In First Out* memory is filled simultaneously to the DA reading the data. The FIFO is read by the micro computer through an interface to the VME bus. A subset of the events taken during a spill period is analysed IN the following interspill period.

During the interspill period all parts of the TOF are controlled by the micro computer. A monitoring program periodically starts various tasks both for the analysis of the spill events, and the laser and pulser calibration and subsequently analyses the calibration data. results consisting of mean values, standard deviations and full Width Half Maximum values of TDC and ADC spectra are read out and recorded on tape by the DA at the end of the next spill and error messages are transferred to the control room.

During the first period of test beam and the later data taking periods the stand alone facility of the detector proved to be reliable and very useful.

## 3 Calibration

### 3.1 Electronic Constants

Most correction constants can be obtained by analysing the interspill data. ADC pedestals are measured during interspill. The conversion factors for TDC counts to seconds are obtained by linear fits to the TDC values for different delay times.

### 3.2 The Time Walk

the discrimination of an analog pulse with constant threshold affects the precision of the time measurements. The Time Walk has been measured and parametrized in dependence to the pulse integral by previous experiments. Our data are well described by [7]:

$$t = \frac{a}{\sqrt{\text{ADC}}} + t_0. \quad (1)$$

Twice per day laser pulses with different intensities are used to measure this effect. The ADC and TDC values of each counter are fitted using equation (1) as shown in figure 3.

### 3.3 The Velocity of Light in the Scintillators

To measure the velocity of light in the scintillators, all counters are supplied with two and some with six feed-in-points for fibers. At each fiber position measurements were carried out using different laser intensities.

Figure 3 shows data points on the two-dimensional correction plane. The straight lines describe the Time Walk at constant vertical position  $z$ . Their gradient  $a$  is the average of many measurements fitted using equation (1). The intercepts of the straight lines show a linear dependence in  $z$ . Consequently the apparent velocity of light in the scintillator is position independent. The average value of all counters was found to be:

$$c_{\text{NE110}} = 16.2 \pm 0.4 \text{ cm/ns}. \quad (2)$$

A similar value was measured in [7] using electrons.

### 3.4 The Synchronization

The synchronization of the different counters of a TOF detector is an important part of the calibration procedure. The Time Walk analysis described above yields the time offset  $t_0$  of the wing counters relative to each other at infinite pulse height.

The overall time offset between wing and reference hodoscopes is determined for high momentum particles as the difference between the calculated ( $\beta \cong 1$ ) and the measured time of flight (figure 4).

### 3.5 The Number of Photoelectrons

For checking purposes, the number of photo electrons reaching the first dynode of the PM can be estimated at sufficient photon statistics by [8]:

$$N = \left( \frac{\langle \text{ADC} \rangle}{\sigma_{\text{ADC}}} \right)^2. \quad (3)$$

$\langle \text{ADC} \rangle$  and  $\sigma_{\text{ADC}}$  are mean value and standard deviation of ADC spectra. The number of electrons is also proportional to the ADC value:

$$N = g \times \text{ADC}. \quad (4)$$

The slope  $g$  is then obtained by combining the relations to:

$$\langle \text{ADC} \rangle = g \times \sigma_{\text{ADC}}^2 \quad (5)$$

and by fitting (5) using laser measurements at different intensities (figure 5).

### 3.6 The Standard Deviation of the Time Measurements

The TOF identification power depends on the actual time resolution which is in turn dependent on the number of photo electrons,  $N$ . It improves with  $1/\sqrt{N}$  [8].

In addition the resolution depends on the slope of the leading edge of the PM pulse crossing the discriminator threshold [3]. Both effects empirically result for our system in a simple dependence of the time resolution on the ADC value of the PM pulse:

$$\sigma_{\text{Time}}(\text{ADC}) = \sigma_0 + \frac{\sigma_1}{\text{ADC}}. \quad (6)$$

In figure 6 the dependence is shown using laser measurements with different intensity. The intercept  $\sigma_0$  and the gradient  $\sigma_1$  are obtained by fitting (6) for each PM.

The time resolution for the physics data processing is determined on a track by track basis to ensure an optimum of identification information.

### 3.7 The Time Drift of the Counters

During running periods, the relative time drift of the individual counters was measured once per hour using high intensity laser light. At these high photon statistics the TDC spectra of the counters have standard deviations of about 100ps. The error of the mean value is then of the order of a few pico seconds. As an example the time drifts of three counters are shown in figure 7 for four weeks of the running period 1990. Possible fluctuations in the laser intensity are suppressed by subtracting the average time measurement of all counters from the individual measurement.

## 4 Reference Counter

For a precise time measurement it is necessary to define a reference time. as the trigger strobe of the experiment does not provide the required accuracy, the time of the incident muon is precisely measured by a reference hodoscope in the beam line, 60m upstream of the target. It consists of a scintillation area divided into five parts, each connected to two photo tubes. It is equipped with the same electronics as the wing hodoscopes and is also supplied with fibers. A more detailed description can be found in [9] or [1].

The electronics are calibrated in the same way as the wing electronics. The measured times are corrected for Time Walk. The correction for the vertical position of a hit is slightly more complicated. The shape of the reference counter elements causes a non constant velocity of light in the scintillators. The function of  $z$  is obtained in the following way: Time spectra for muons passing different  $z$  positions are measured. The mean values of these distributions are then fitted by a polynomial in  $z$ .

In figure 8 the difference of time measurements of two overlapping counters for a track passing both is shown. The resulting resolution for a single counter is:

$$\sigma_{\text{Ref}} = 140\text{ps.} \tag{7}$$

## 5 Electron Calibration Data

In November 1987, the experiment E665 collected calibration data with electron and positron beams. Electrons and positrons of momenta in the range of 2 to 7 GeV/ $c$  were found to be in the acceptance of the TOF. The true time of flight for a path length  $l$  is here in good approximation:

$$t_{\text{Truth}} = l/c. \quad (8)$$

For a single counter the path length is almost constant. Electron time spectra of individual counters therefore provide the possibility to calculate a realistic estimate for the time resolution achieved.

In figure 9 the influence of different correction steps applied to the time measurements is shown. The TDC values of the top and bottom tubes of a counter are converted to seconds and the relative time offset  $t_0$  (1) of the individual tube is subtracted.

The spectrum drawn with a dotted line shows the average of the times of top tube  $t_{\text{Top}}$  and bottom tube  $t_{\text{Bot}}$ . With constant velocity of light in the scintillator the corrections for  $z$  cancel:

$$\begin{aligned} t_1 &= \frac{1}{2} \left( \left( t_{\text{Top}} + \frac{z}{c_{\text{NE110}}} \right) + \left( t_{\text{Bot}} - \frac{z}{c_{\text{NE110}}} \right) \right) \\ &= \frac{1}{2} (t_{\text{Top}} + t_{\text{Bot}}). \end{aligned} \quad (9)$$

The next distribution (dashed line) is much narrower. The time of the incident particle measured by the reference counter (corrected for  $z$  and Time Walk) is subtracted for each electron track. This removes the disturbance due to the trigger timing:

$$t_2 = \frac{1}{2} (t_{\text{Top}} + t_{\text{Bot}}) - t_{\text{Ref}}. \quad (10)$$

A final improvement is achieved by correcting top and bottom times for Time Walk:

$$t_3 = \frac{1}{2} (t_{\text{Top}} + t_{\text{Top}}^{\text{Time Walk}} + t_{\text{Bot}} + t_{\text{Bot}}^{\text{Time Walk}}) - t_{\text{Ref}}. \quad (11)$$

In figure 10 time resolutions of different counters are displayed. The error bars reflect the number of electron hits in individual counters. As a comparison, also the time resolution calculated according to (6) is shown (line).

The overall time resolution  $\langle \sigma_{\text{Electron}} \rangle$  of the TOF detector was calculated as an average of the time resolution of the individual counters weighted with the electron statistics:

$$\langle \sigma_{\text{Electron}} \rangle = 225 \text{ps}. \quad (12)$$

## 6 Conclusion

The TOF detector described in this article is provided with devices for permanent documentation and checking of all functions.

This is made possible by a laser calibration system. Constants describing systematic effects on time measurements are calculated from calibration data. The synchronization of the individual counters is obtained from the laser calibration system. In addition, the number of photo electrons per ADC counts is fitted using laser data and the dependence of the standard deviation of the time measurement on the number of photo electrons is parametrized.

The quality of the corrections applied was checked using an electron test beam. The overall mean time resolution for electrons was determined to be 225ps.

## Acknowledgements

We want to thank H. v. d. Schmidt (University Bonn) for the support in using the ACCI. R. Borst provided the knowledge about the VME bus.

## References

- [1] M. R. Adams et al., NIM A291 (1990) 533
- [2] M. Erdmann, PhD Thesis, University Freiburg (1990)
- [3] M. Erdmann, Diploma Thesis, University Freiburg (1985)
- [4] C. Jacobs et al., CERN CAMAC Note 63-00 (1976),  
C. Jacobs et al., CERN CAMAC Note 64-00 (1976)
- [5] H. v. d. Schmidt, private communication, University Bonn (1983)
- [6] U. Seidler, internal note, University Freiburg (1988)
- [7] W. Braunschweig et al., NIM 134 (1976) 261
- [8] G. Pietri, Proc. of Int. Conf. on Instrumentation for HEP, Frascati (1973) 586
- [9] M. Wilhelm, Diploma Thesis, Freiburg (1988)

## Figure Captions

1. Distributing the UV light into the scintillators
2. TOF electronics
3. Two dimensional correction plane for hits generated with a fiber connected to the counter at various distances from the top photomultiplier
4. Inverse flight velocity versus momentum of particles for data (all corrections applied). The lines represent true values for different types of particles.
5. Correlation between mean values and squares of standard deviations of laser ADC spectra. The straight line is given by a linear fit, the gradient is the number of Photo electrons par ADC count.
6. Standard deviation of time measurement versus inverse ADC mean value; laser data, with a linear fit
7. The time drift of typical counters over a period of four weeks during 1990
8. A time spectrum of the reference hodoscope for muons. The values are differences of two measurements for the same track, with a gaussian fit.
9. Time spectrum of a single counter in electron data. The distributions show the effect of different corrections applied to the data.
10. The time resolution of several counters measured with electrons

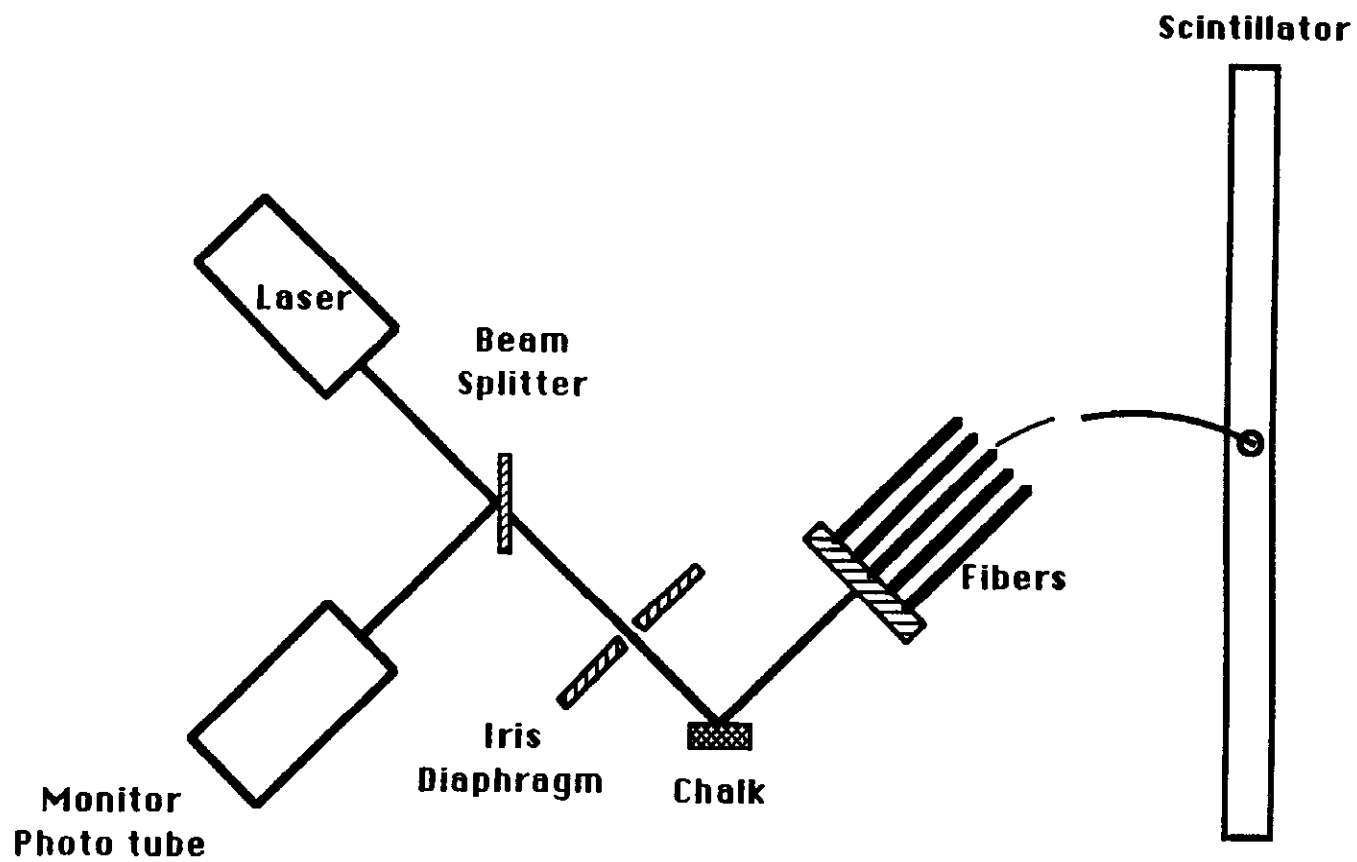
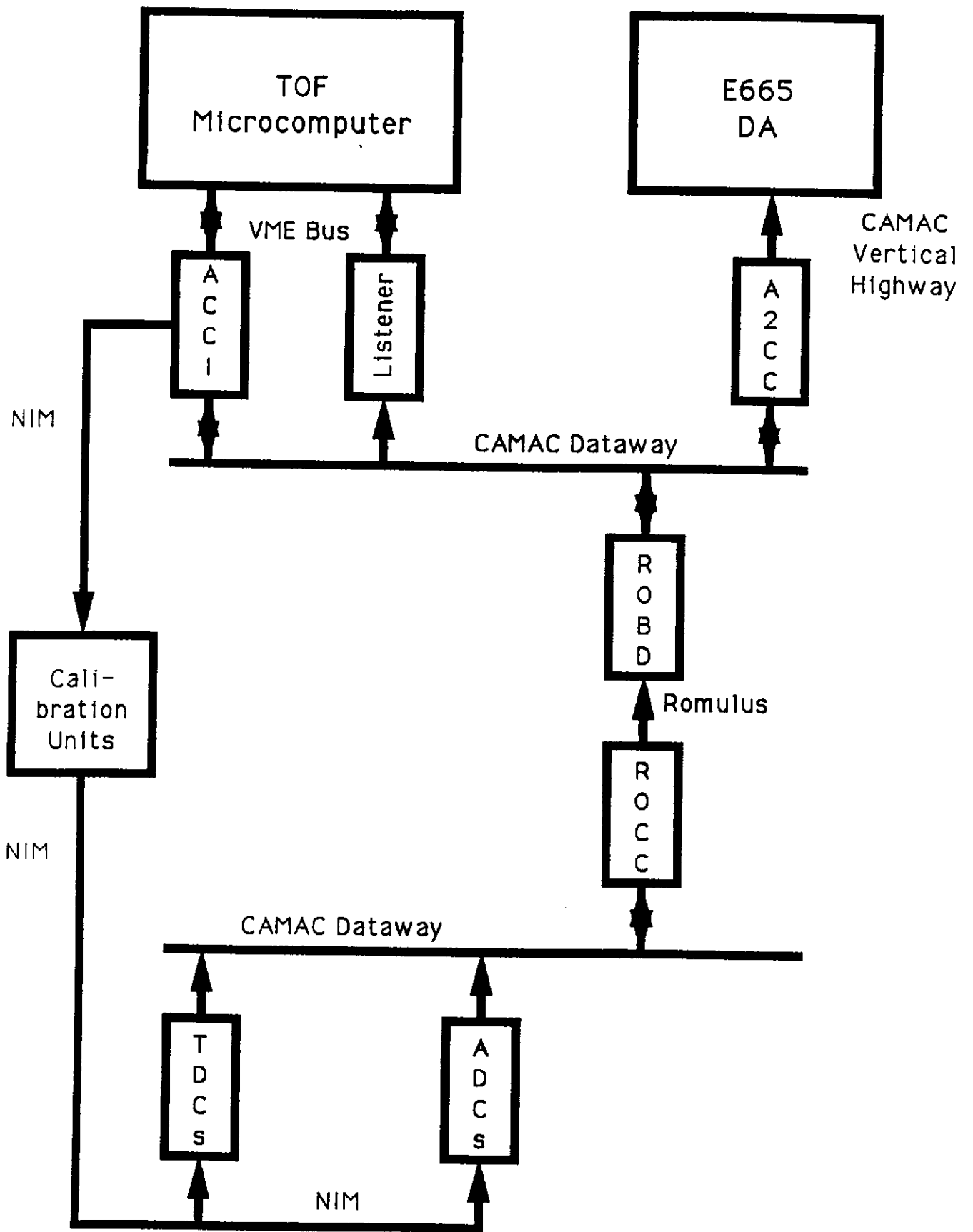


Figure 1

Figure 2



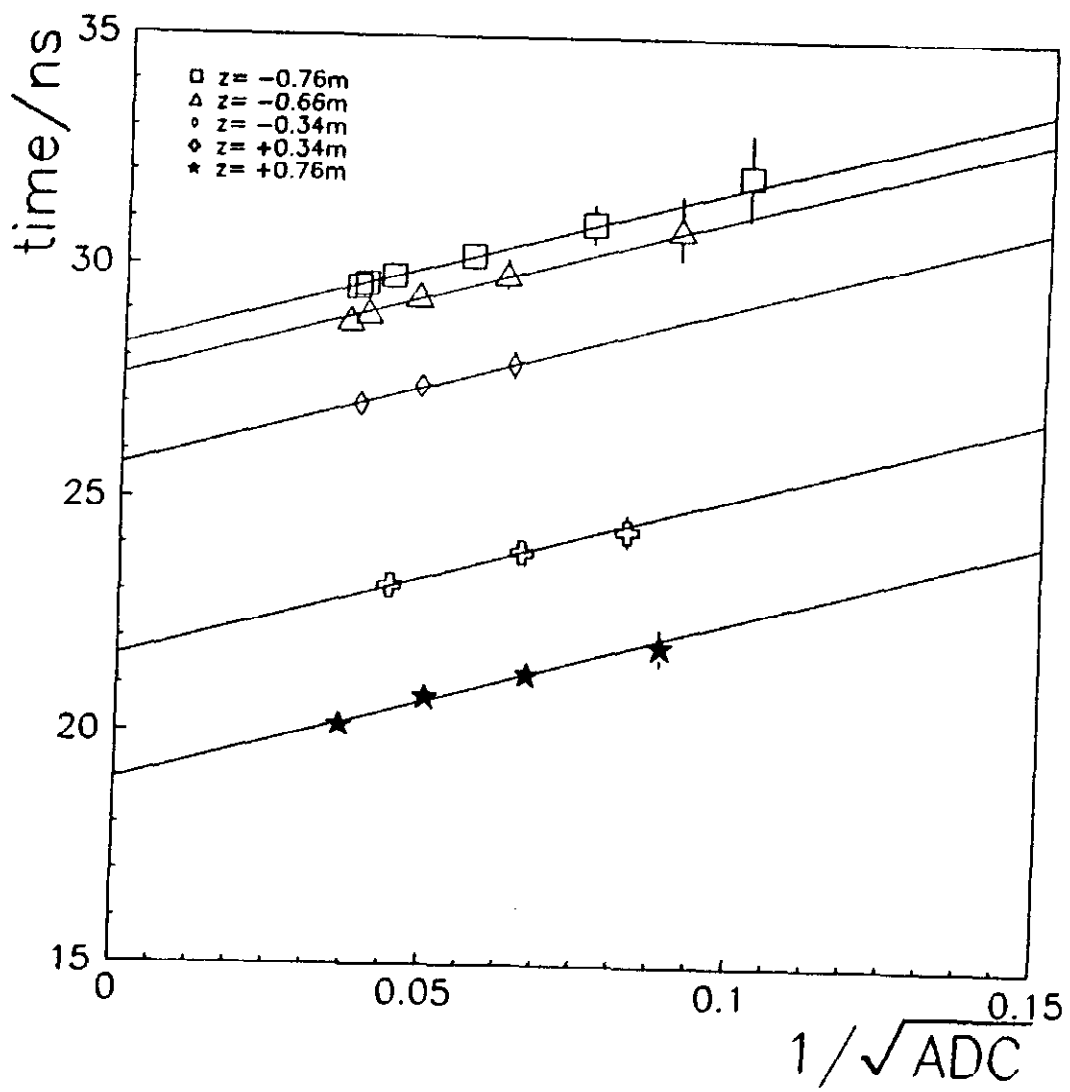


Figure 3

Figure 4

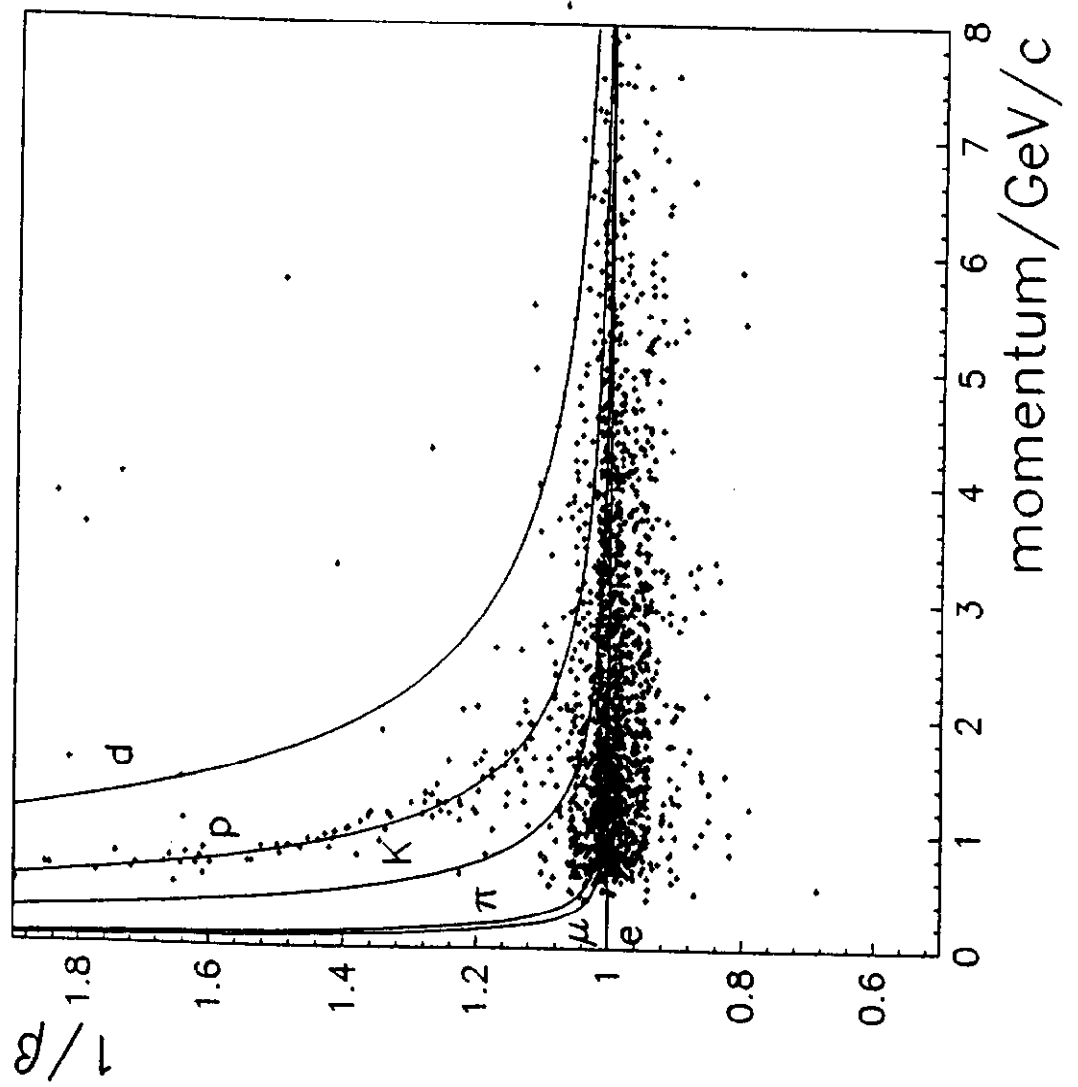


Figure 5

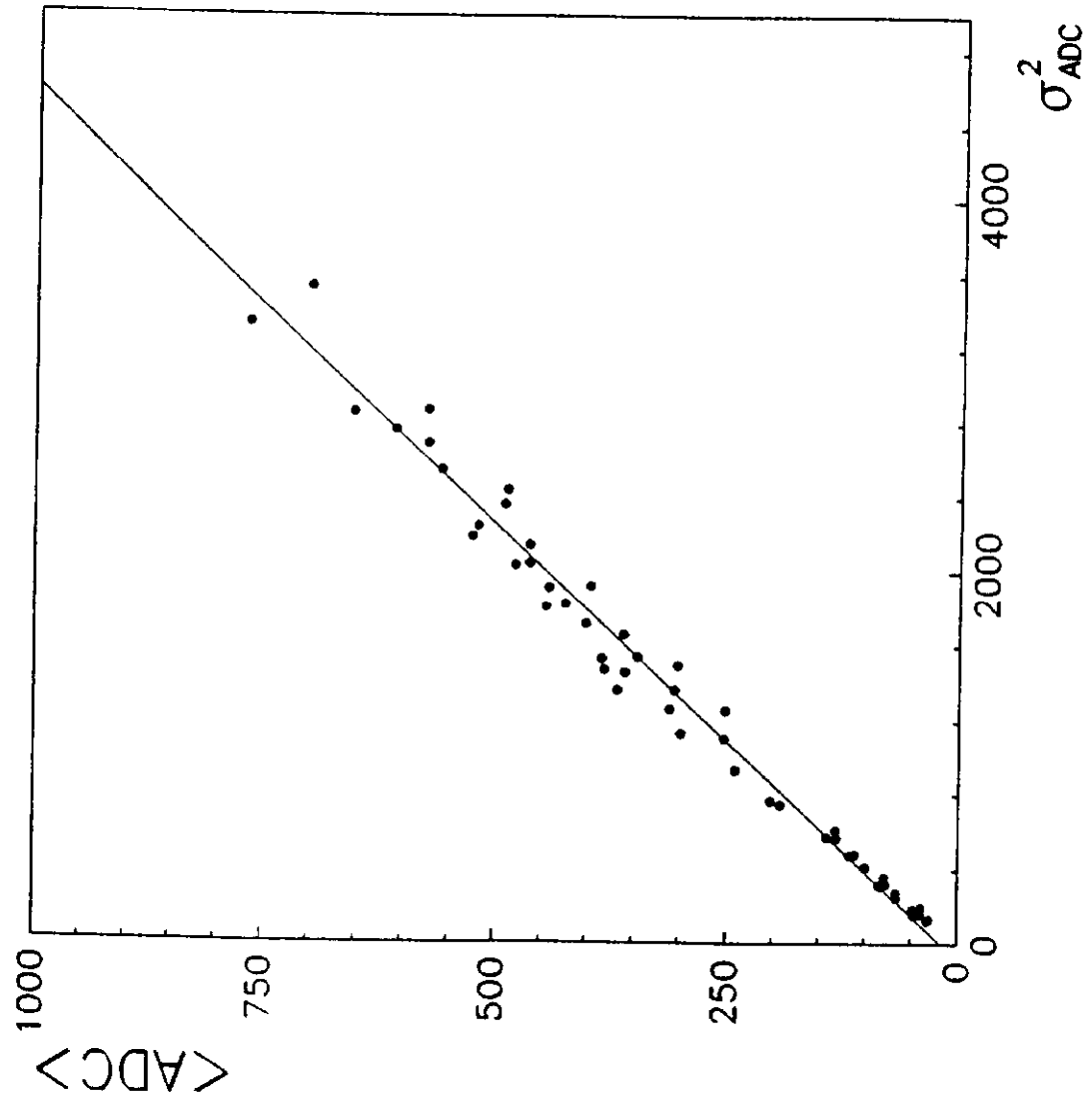


Figure 6

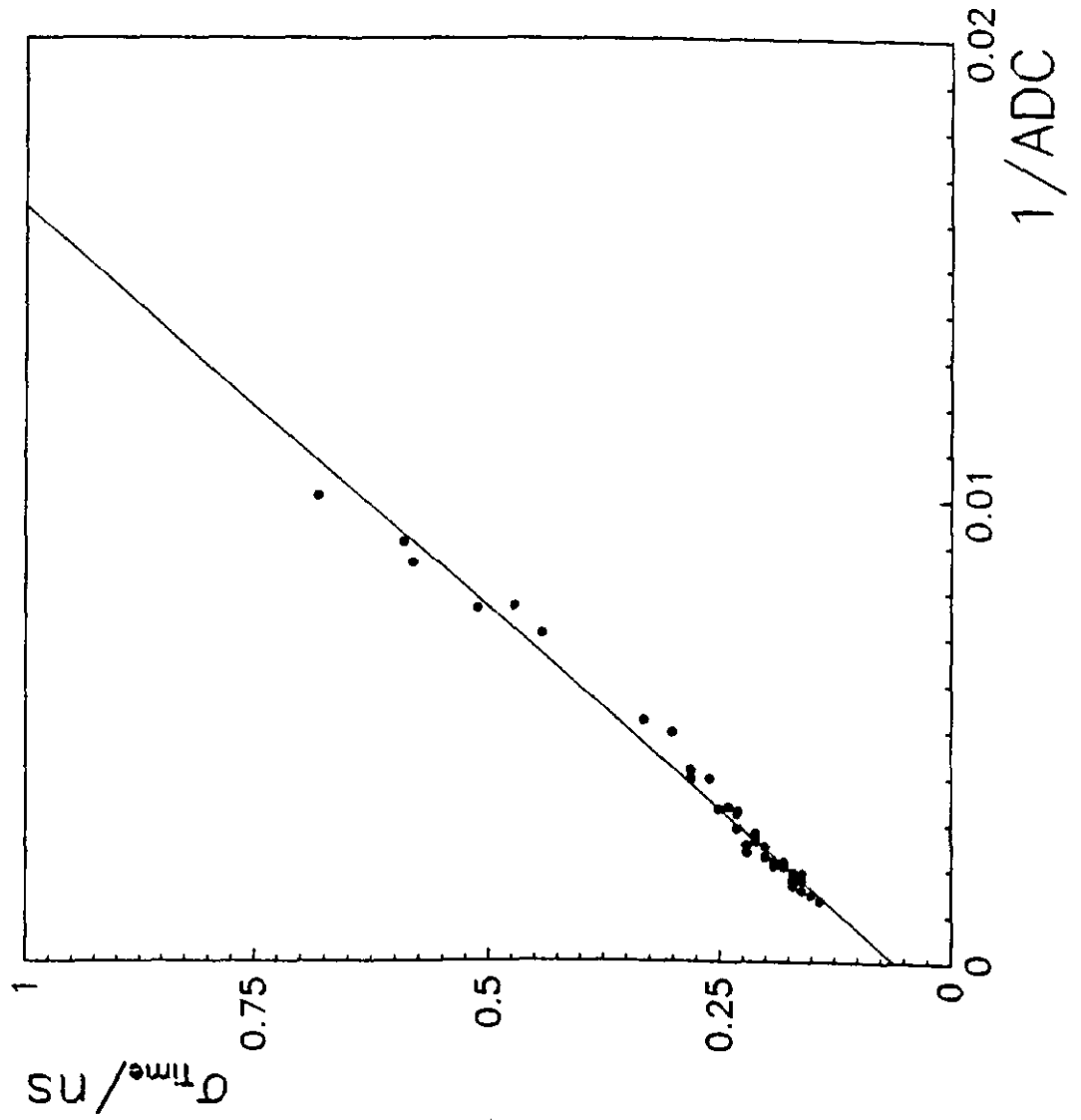


Figure 7

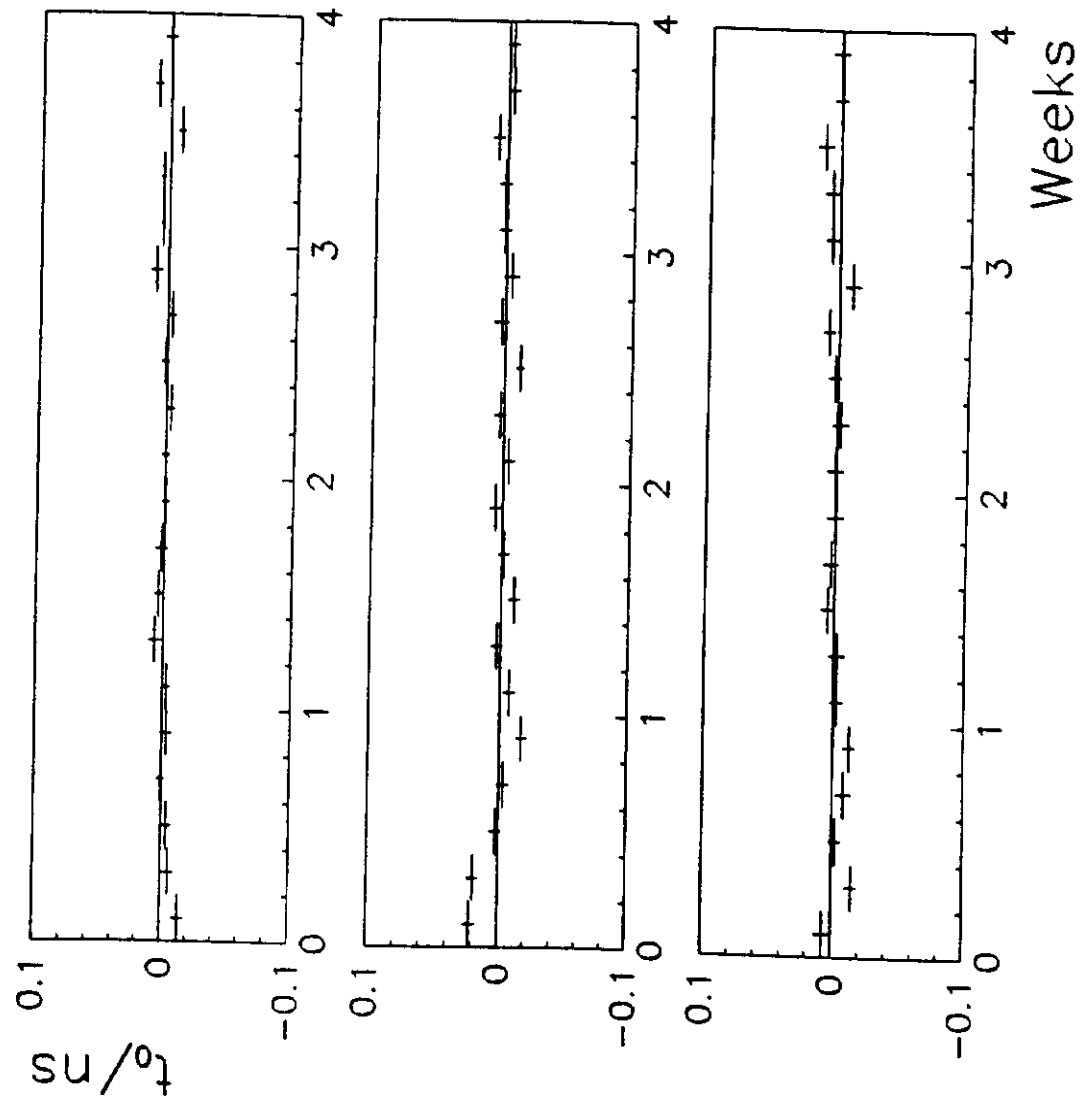


Figure 8

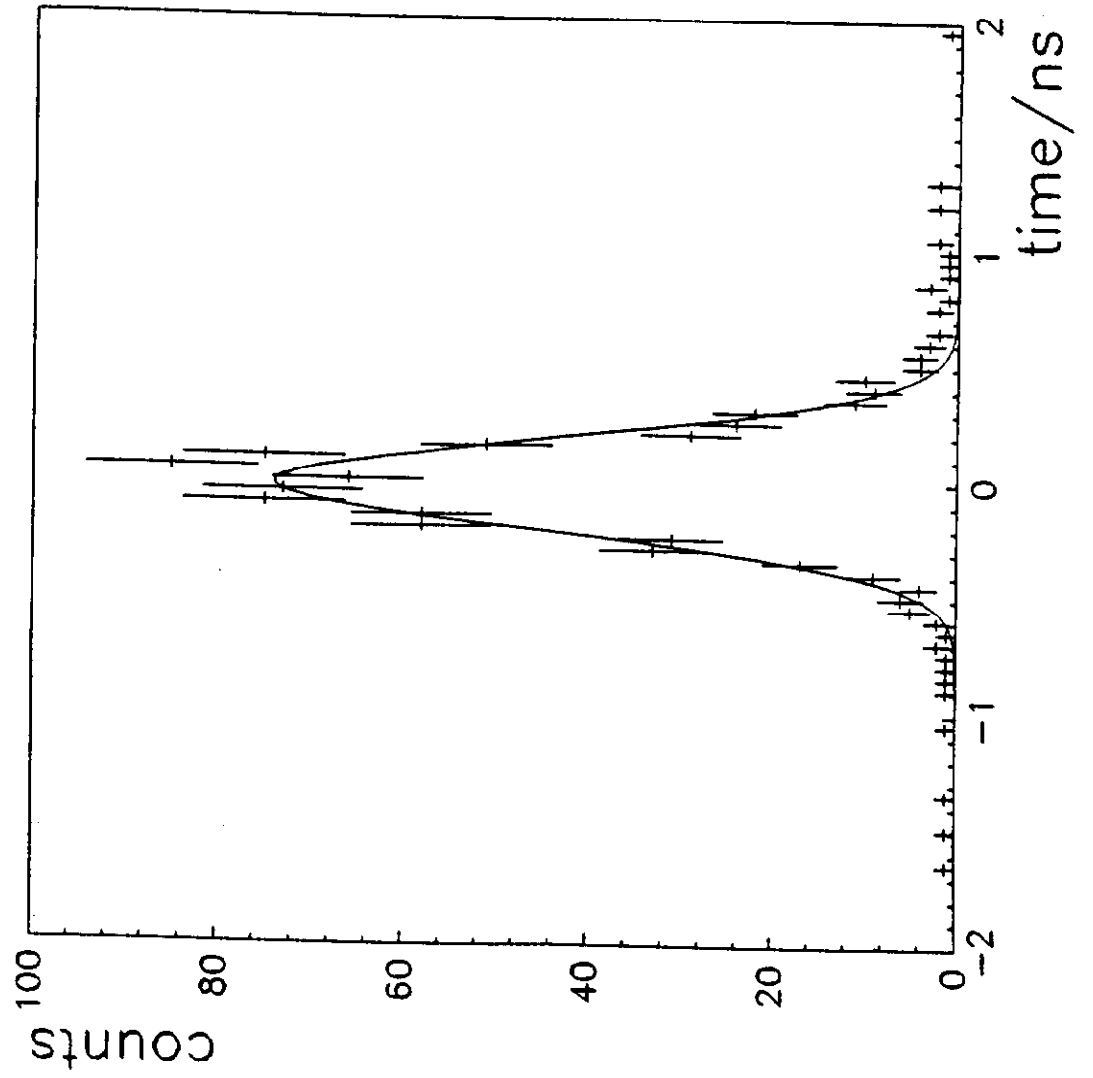


Figure 9

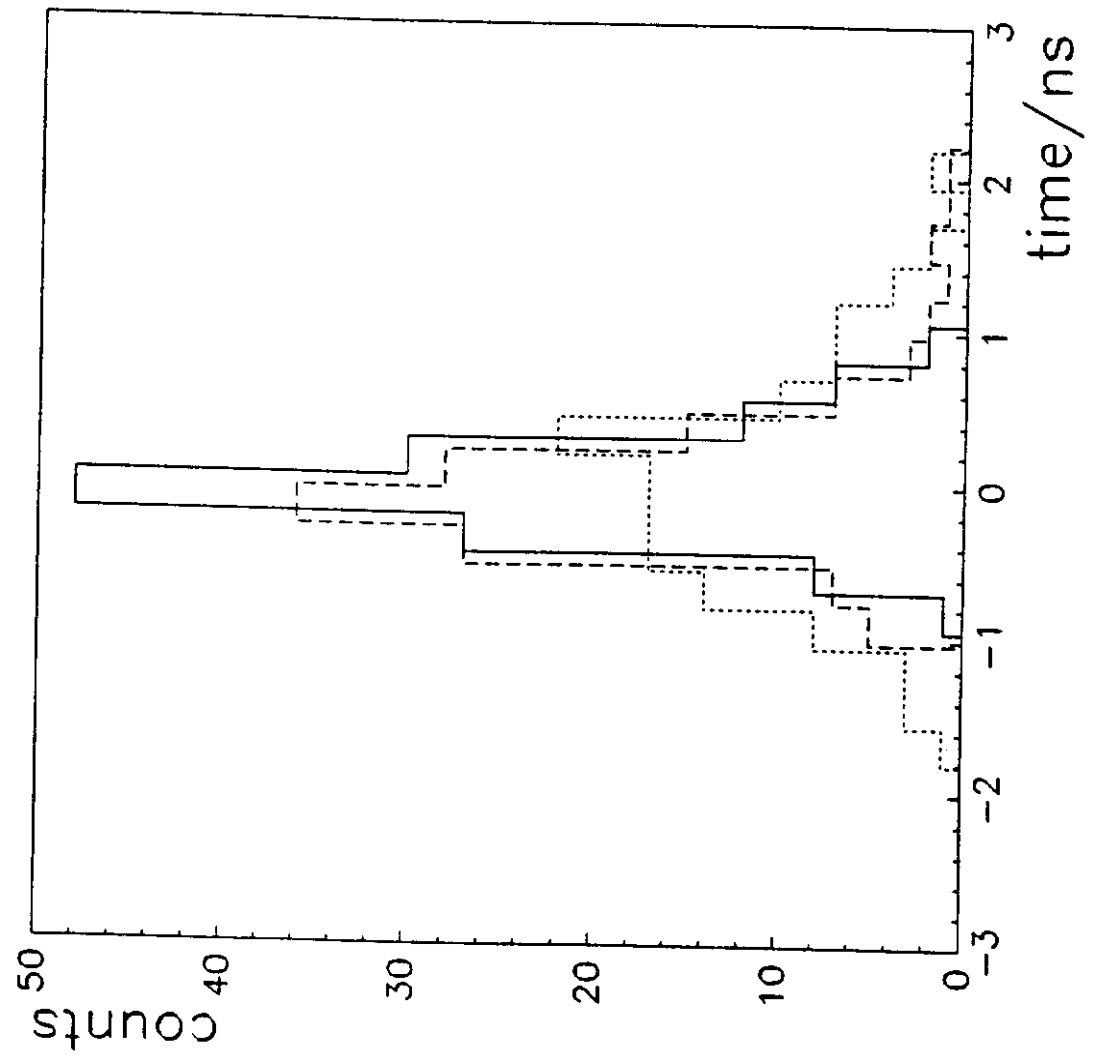


Figure 10

